Structure Development during Dry–Jet–Wet Spinning of Acrylonitrile/Vinyl Acids and Acrylonitrile/Methyl Acrylate Copolymers

P. Bajaj, T. V. Sreekumar, K. Sen

Department of Textile Technology, Indian Institute of Technology, Delhi, Hauz Khas, New Delhi 110016, India

Received 20 February 2001; accepted 12 January 2002

ABSTRACT: Dry–jet–wet spinning of three copolymers, poly(acrylonitrile/methyl acrylate), poly(acrylonitrile/methacrylic acid), and poly(acrylonitrile/itaconic acid), was performed with a dimethylformamide/water (60:40 v/v) coagulation bath at different temperatures (10–40°C). The fibers were stretched to different levels (1.1–6×) in boiling water, collapsed, and annealed over a heater plate at 130°C. The effects of the polymer composition, coagulation bath temperature, and draw ratio on the cross-sectional morphology, structure, and tensile properties are reported. The cross-sectional shape of the gel fibers underwent a transition from a kidney shape to an oval shape, and macrovoids began to appear at higher temperatures. However, F(AN/IA) gel fibers changed from a kidney shape to an irregular shoe type with a gel network of interconnected polymer fibrils. For F(AN/MAA) gel fibers, the diameter increased from 45 to 67 μm when the coagulation bath temperature was increased from 10 to 40°C, and the denier value decreased from 17.5 to 14.3 den/filament. The strength, modulus, and elongation at break decreased with an increase in the coagulation bath temperature. For F(AN/MAA) fibers coagulated at 10°C in a spin bath, the strength increased from 0.43 to 2.213 g/den, the modulus increased from 27 to 76 g/den, and the density increased from 1.177 to 1.196 g cm^{-3} when the gel fibers were drawn to 6×. However, 6× drawn F(AN/MA) fibers had a higher strength (3.1 g/den) and elongation (14.6%) in a 40°C coagulation bath. F(AN/IA) fibers could be drawn only to a draw ratio of 4× instead of the 6× draw ratio for F(AN/MAA) and F(AN/MA) fibers. Therefore, the final F(AN/IA) fibers exhibited poor mechanical properties (tenacity = 0.81 g/den, modulus = 22 g/den, and elongation at break = 8%). The crystallinity did not change significantly (χ_c = 61–63%) with the draw ratio, but the crystal size increased from 22.9 to 43.4 Å and orientation factor from 0.41 to 0.78. The dichroic ratio, measured with Fourier transform infrared, decreased with an increase in the draw ratio, but the sonic modulus and crystalline orientation values increased with an increase in the draw ratio. Thermomechanical data show a maximum physical shrinkage of 51.7% for 6× drawn F(AN/MA) and a minimum physical shrinkage of 30.5% for 4× drawn F(AN/IA) fibers. J Appl Polym Sci 86: 773–787, 2002

Key words: acrylic fibers; dry–jet–wet spinning; polyacrylonitrile; wet spinning; coagulation; drawing; heat setting

INTRODUCTION

Acrylic fibers are produced with dry, wet, and dry–jet–wet spinning methods.[1–6] In wet spinning, coagulation is the key process in which the polymer solution (dope) is converted into gel fibers because of the phase separation of the dope in a solvent/nonsolvent mixture.[7] Counterdiffusion of the solvent from the dope and counterdiffusion of the nonsolvent from the coagulation bath take place simultaneously but may occur at different rates, which depend on the coagulation bath composition and temperature.[8]

Various factors that influence the coagulation process include the polymer composition, dope solid, coagulation bath composition, coagulation bath temperature, and jet stretch.

Polyacrylonitrile (PAN) homopolymer is generally not used for fiber spinning because its copolymers are more soluble and make the preparation and storage of the spinning dope much easier. The resulting fibers from copolymers are also more extensible and less prone to fibrillation.[1] Dope made from PAN homopolymer gels very quickly, but the addition of comonomers tends to decrease the gelation rate and make the dope easier to handle.

Prasad[9] observed that with a reduction in the dope viscosity the extension and spinning speed could be increased. Gelation increases the dope viscosity and may adversely affect the extrusion speeds. The production of acrylic fibers from copolymers containing acrylonitrile (AN), methyl acrylate (MA) and acrylic acid (AA), or methacrylic acid (MAA) in 51.5% aqueous solutions of sodium thiocyanate was studied by Mamazhanov et al.[10] It was observed that an increase in AA or MAA of up to 6 wt % in the copolymer had

Correspondence to: T. V. Sreekumar, School of Textile and Fiber Engineering, Georgia Institute of Technology, Atlanta, GA 30318 (sreekumar.veedu@textiles.gatech.edu).

hardly any effect on the physicomechanical properties of the fibers. The synthesis of AN copolymers containing MAA and itaconic acid (IA) via dimethylformamide (DMF)/water suspension polymerization has been reported.[11] A number of references can be cited for the production of AN copolymers containing MAA, AA, IA, MA, and so forth.[12–14]

The solid content in the dope plays an important role in fiber morphology and density.[8] Increasing the polymer concentration improves the homogeneity of the fiber structure by reducing the incidence of larger voids. As a result, the gel fiber density also increases.

Takahashi et al.[15] investigated the effects of different solvents, nonsolvents, and their ratios in the coagulation bath on fiber structure and properties. The PAN used in their work was reported to have an intrinsic viscosity ([η]) of 1.65 dL g^{-1}. It was pointed out that the properties of undrawn filaments obtained via spinning into a dimethyl sulfoxide (DMSO)/H_2O solution were very different from those of the filaments obtained via spinning into carbon tetrachloride or methanol spinning baths. The former was reported to show larger voids, a higher degree of water retention, and a larger small-angle scattering power. The number of voids decreased when the DMSO concentration increased from 0 to 70% in the coagulation bath.

The coagulation bath temperature is one of the most important factors determining the morphology and properties of acrylic fibers. The effect of the coagulation bath temperature on the structure morphology of AN-based fibers has been reported by various researchers.[8,16,17] When the coagulation bath temperature is increased, the cross-section shape undergoes a transition from a kidney shape to a round shape, and macrovoids begin to appear at higher temperatures. Bajaj and Kumari[18] also observed the formation of a skin–core structure when a dope of a terpolymer containing AN (92.7%), vinyl acetate (7%), and sodium methallyl sulfonate (0.3%) with [η] = 1.14 dL g^{-1} was wet-spun into a coagulation bath consisting of 45:55 dimethylacetamide/H_2O at 60°C. The mechanism by which the reduced bath temperature (5–10°C) gives improved fiber structure properties has always been related to the coagulation rates. At low temperatures, coagulation is retarded, and more time is available for an internal adjustment of osmotic stresses. In addition, slower coagulation results in less skin formation, and this, in turn, leads to smaller and fewer voids. As far as the cross section is concerned, at low coagulation temperatures, the outward diffusion of the solvent predominates, giving rise to bean- or kidney-shaped cross sections. However, at higher temperatures, coagulation takes place by counterdiffusion of the solvent and nonsolvent.

The coagulation process is also dependent on the jet stretch, which is the ratio of the first godet take-up velocity to the theoretical polymer dope velocity at the exit of the capillary. The effect of jet stretch on the fiber properties is primarily exhibited in luster and dry–collapse–relax processes. Low jet stretch (≈0.5) conditions produce smaller void structures that are more transparent to light, lustrous, and easily collapsible. However, the effect of jet stretch is not observed on the tensile properties[19] after the acrylic fibers are stretched, dried, collapsed, and relaxed.

Unlike wet spinning, in dry–jet–wet spinning, the dope is extruded through an air gap of less than 1 cm, and this is followed by coagulation by a conventional method, which can overcome some of the shortcomings of wet-spinning technology. This has the advantage of allowing the extruded dope to cool to a certain extent in the air gap before reaching the coagulation bath and also to relax the high stresses developed inside the spinnerette assembly. Baojan et al.[20] found a milder coagulation for dry–jet–wet spinning and demonstrated the possibility of a higher spinning speed in comparison with wet spinning. A patent to Nikkiso Co., Ltd.,[21] describes the development of high-strength acrylic fibers spun from a terpolymer, poly(acrylonitrile/methyl acrylate/itaconic acid) (98:1:1). Dope containing a 5% solid content was extruded in air and passed through a coagulation bath. Fibers were drawn to a draw ratio of 6, washed, and lubricated. Final drawing of the fiber gave fibers with a tensile strength of 78 kg/mm^2.

In addition to spin orientation, the subsequent drawing of acrylic fibers causes molecular orientation along the fiber axis. This leads to an increase in the mechanical properties. Kumar and Stein[22] observed a decrease in the dichroic ratio with an increase in the draw ratio when copolymer fibers of poly(acrylonitrile/methyl acrylate) (75/25) were drawn to different draw levels. Unlike other synthetic fibers, for stretched AN polymer fibers, all functional groups (C≡N, C═O, etc.) except carbon chains lie perpendicular to the chain axis. Therefore, in a drawn fiber the absorption of plane-polarized IR rays will be more in the perpendicular direction. Therefore, the ratio of parallel absorption to perpendicular absorption will be low in comparison with that of undrawn fibers. Paul[23] also reported that fibers produced from poly(acrylonitrile/vinyl acetate) (92.3:7.7 w/w) at a higher draw ratio showed a higher orientation factor, as measured by both sonic modulus and wide-angle X-ray diffraction (WAXD). Bell and Dumbleton[16] found a significant decrease in the half-width of the X-ray peak at 17.2° ($\beta_{1/2}$) with an increase in the draw ratio. When the half-width of 2× drawn fiber is 52, that of 8× drawn fiber is 27. In the same way, the strength of fibers also increases with the draw ratio because of orientation.

In this article, the effects of the polymer composition, coagulation bath temperature, and stretch ratio

TABLE I
Characterization of AN Copolymers

Copolymer	Comonomer content (mol %)	[η] (dL/g)	Dope solids in DMF (wt %)
P(AN/MAA)	1.3	2.50	14.2
P(AN/MA)	1.3	2.53	12.6
P(AN/IA)	0.7	2.50	14.3

on the structure properties of acrylic fibers produced by dry–jet–wet spinning are reported.

EXPERIMENTAL

Materials

Three copolymers of AN with MAA, MA, or IA were synthesized by DMF/water suspension polymerization. The details of the polymerization are given elsewhere.[11] Characteristics of the polymers are given in Table I.

Dope preparation

The polymer solution (dope) was prepared by the dissolution of finely powdered, dried polymer in DMF at less than 5°C (ice cold water); this yielded a solid content of 12.5–14.5 wt %. The whole mixture was stirred until a clear solution was obtained. Subsequently, it was deaerated in vacuo at 70°C for the removal of air bubbles and was filtered through a stainless steel mesh before spinning.

Brookfield viscosity

The Brookfield viscosity was measured on a Brookfield RVTD digital viscometer with a temperature setting arrangement and with a cylindrical spindle (29 BS) at 20 rpm and at different temperatures varying from 40 to 100°C:

$$\text{Viscosity (centipoise)} = \frac{\text{Shear stress} \times 100}{\text{Shear rate}}$$

Dry–jet–wet spinning

The fiber spinning was carried out on a spinning machine supplied by Bradford University Research, Ltd. (Fig. 1), with a 500-hole spinneret with 50-μm hole diameter. The air gap between the jet and the coagulation bath was kept at 3 mm. The ram speed and first take-up roll speed were kept at 1 mm/min and 1 m/min, respectively. The volumetric throughput rate (Q) was adjusted at

$$Q = 3.84 \times 10^{-3}\ \text{ml/min/hole}$$

Now, the average jet velocity was calculated as

$$\langle V \rangle = \frac{Q}{\pi r^2}$$

where r is the radius of the spinneret hole (cm). Therefore,

$$\langle V \rangle = \frac{3.84 \times 10^{-3}}{3.14 \times (50/2 \times 10^{-4})^2}$$

$$= 195.67\ \text{cm/min}$$

The take-up roll speed (V_1) was 100 cm/min. Therefore, the jet stretch was equal to

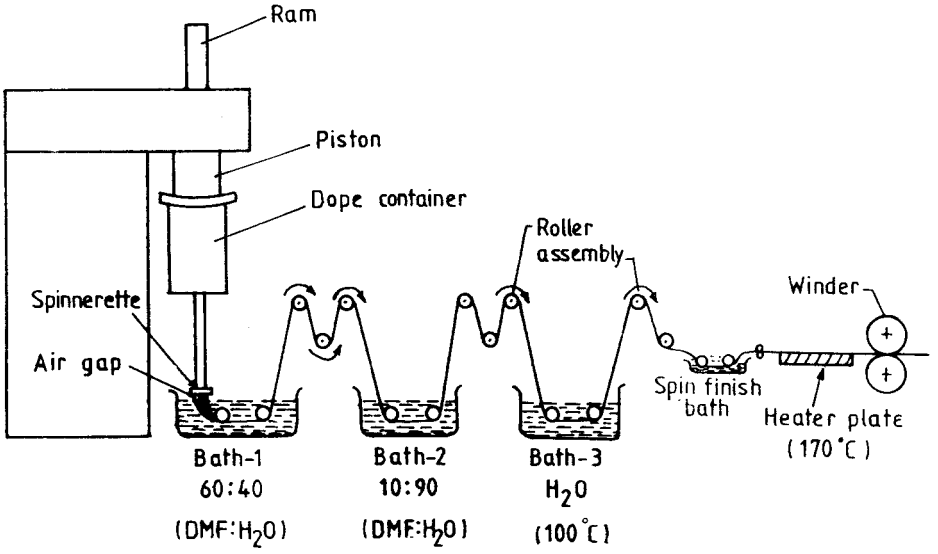

Figure 1 Laboratory spinning line.

TABLE II
Spinning Conditions of AN Copolymers

I Bath/coagulation bath		
Composition	60/40 DMF/H_2O	
Temperature	10, 20, 30, or 40°C	
Throughput rate	3.84×10^{-3} mL/hole/min	
Jet stretch	0.5	
Residence time in the bath	48 s	
Take-up roller speed	1 m/min	
II Bath		
Composition	10/90 DMF/H_2O	
Temperature	40°C	
Residence time	43 s	
Take-up roller speed	1.1 m/min	$\lambda_1 = 1.1$
III Bath		
Composition	0/100 DMF/H_2O	
Temperature	98 ± 2°C	
Residence time	14 s	
Drying and collapsing		
Heater plate length	50 cm	
Heater plate temperature	130°C	
Winding speed	4–6 m/min	$\lambda_2 = 5.5$
Total draw ratio	$\lambda_1 \times \lambda_2 = 1.1 \times 5.5 = 6$	

λ = draw ratio. In the case of P(AN/MAA), we adjusted the total draw ratio at 4, 5, and 6 by adjusting the draw in the third bath.

$$\therefore \text{Jet stretch} = \frac{V_1}{\langle V \rangle} = \frac{100}{195.67} = 0.51$$

The spinning conditions are given in Table II.

WAXD

X-ray diffraction of the powdered specimens was obtained on a Phillips PW1710 X-ray diffractometer with nickel-filtered Cu Kα radiation at a 1° scan rate. For orientation measurements, the fiber samples were wound on an aluminum sample holder in such a manner that the individual filaments were parallel. The 2θ angle of 16.9° was used to determine the fiber orientation. With 2θ set at 16.9°, an azimuthal scan was taken.

The crystallinity (χ_c) of the samples was calculated with the following equation:

$$\chi_c = \frac{A_c}{A_a + A_c} \times 100 \quad \text{(i)}$$

where A_c and A_a are the areas under the crystalline and amorphous curves, respectively. The average crystal size (t_c) and inter planar d-spacing were calculated with the Scherrer equation and the Bragg equation, respectively

$$t_c = \frac{K\lambda}{\beta \cos \theta} \quad \text{(ii)}$$

$$n\lambda = 2d \sin \theta \quad \text{(iii)}$$

where $\lambda = 0.154$ nm is the wavelength of the X-ray used, K is the apparatus constant (0.89), β is the half-width (rad) of the X-ray diffraction peak, and θ is the Bragg angle at which maxima of the diffraction curves appear.

The width in degrees of the half-maximum intensity ($\beta_{1/2}$) of the peak obtained from an azimuthal scan was used to calculate the index of orientation (IO):

$$\text{IO} = \frac{180 - \beta_{1/2}}{180}$$

The lower $\beta_{1/2}$ is, the higher the degree of orientation will be.

Density measurements

Density was measured with a density gradient column (Davenport, London, England) consisting of a mixture of n-heptane and carbon tetrachloride at 25°C. The density was measured 48 h after the introduction of the samples to the column so that equilibrium could be achieved.

Fourier transform infrared (FTIR) spectroscopy

FTIR spectra of the fibers collected from coagulation, washing, and stretching baths were recorded on a Jasco micro FTIR 200 spectrometer. For the determination of the dichroic ratio (D), IR spectra were recorded for each sample, one with the electric vector polarized parallel to the stretching direction and an-

other with the electric vector polarized perpendicular to the stretching direction. Two background scans with two different positions of the polarizer were also taken. $A_{\parallel}$ and $A_{\perp}$ at 2939, 2240, and 1732 cm^{-1} due to $\sqrt{CH_2}$, $\sqrt{C{\equiv}N}$, and $\sqrt{C{=}O}$, respectively, were recorded, where $A_{\parallel}$ and $A_{\perp}$ are the absorbances parallel and perpendicular to the stretch direction. D is given as follows:

$$D = \frac{A_{\parallel}}{A_{\perp}}$$

Sonic modulus

The sonic modulus of the fibers was measured on a pulse propagation meter (PPM 5R) so that we could get an idea about the overall orientation. A single filament was mounted between two transducers containing a piezoelectric ceramic crystal with a natural frequency of 5 kHz. By measuring the transit time of a sonic pulse between the two transducers in contact with the fiber sample, we measured the velocity of a longitudinal wave in the material. Pulses were transmitted at a continuous rate, and timing was also done on that basis; this provided a continuous readout on a strip chart recorder.

Therefore, the velocity calculations were made with length and time measurements taken from the chart recorder:

$$C = \frac{\Delta l}{\Delta t}$$

where C is the sound velocity (km/s). The sonic modulus is represented as

$$E = \rho C^2$$

where ρ is the density (g cm^{-3}). Moreover,

$$\text{E in grams/denier} = C^2K$$

where K is a conversion factor of 11.3. The sonic modulus orientation factor ($\propto$) of a given fiber was calculated by the method given by Paul:[24]

$$\alpha = (E_f - E_g)/E_f$$

where E_f is the sonic modulus of a given drawn fiber and E_g is that of the gel fiber.

Scanning electron microscopy (SEM)

The cross sections of the fibers were studied with a scanning electron microscope (Cambridge Stereoscan 360). Ultrathin cross sections were made and mounted on a stub and coated with silver. They were then scanned, and SEM photographs were taken at magnifications of 400–1000×.

TABLE III
Effect of Solid Content on the Dope Viscosity of P(AN/MA) Copolymer at 70°C, at a Spindle of 29 BS, and 20 rpm

Polymer	Solid content (wt %)	Brookfield viscosity (cP)
P(AN/MA)[a]	14.5	7750
	13.5	6800
	12.5	5700
	11.5	3800

[a] $[\eta]$ = 2.53 dL/g.

Mechanical properties

Mechanical properties of the single filaments were measured on an Instron model 4301 tensile tester under standard conditions (i.e., relative humidity = 65 ± 2%, temperature = 27 ± 2°C) with a gauge length of 25 mm and a crosshead speed of 10 mm/min.

Thermomechanical analysis (TMA)

TMA studies were carried out on a TMA 7 module of a PerkinElmer Delta series thermal analyzer at a heating rate of 10°C/min. A pretension of 40 mN was applied. The test was carried out from 50 to 350°C under a nitrogen atmosphere.

RESULTS AND DISCUSSIONS

Rheological behavior

The dope viscosity of poly(acrylonitrile/methyl acrylate) [P(AN/MA)], poly(acrylonitrile/methacrylic acid) [P(AN/MAA)], and poly(acrylonitrile/itaconic acid) [P(AN/IA)] copolymers of different solid contents in DMF was measured at different temperatures. The viscosity of the dope depended on both the solid content and the temperature (Tables III and IV). A 14.5 wt % solution of P(AN/MA) at 70°C showed a viscosity of 7750 cps. When the solid content was reduced to 11.5 wt %, the viscosity was reduced to 3800 cps. Comparing the viscosities of 14.5 wt % solutions of various copolymers at 70°C, we can see that P(AN/MA) showed a maximum viscosity of 7750 cps and P(AN/IA) showed a minimum viscosity of 4550 cps (Table IV), even though all three copolymers had similar values of $[\eta]$ (2.5–2.53 dL g^{-1}). On the basis of the hydrodynamic volume of three copolymers with MA, MAA, and IA comonomers, we can say that the largest hydrodynamic volume of the IA moiety in the P(AN/IA) copolymer could lead to a lower compactness:

TABLE IV
Brookfield Viscosity (cP) of AN Copolymers at Different Temperatures

	Solid content		
Temperature	P(AN/IA) 14.5%	P(AN/MAA) 14.5%	P(AN/MA) 12.6%
40	13,750	14,350	13,500
50	9,500	10,600	10,050
60	6,250	8,250	7,500
70	4,550	6,200	5,700
80	3,200	5,000	4,400
90	2,300	3,950	3,250
100	1,800	2,950	2,600

MA : $CH_2 = CH- COOCH_3$

MAA :

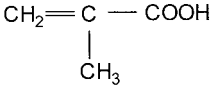

IA :

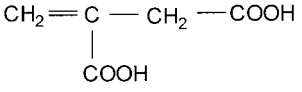

However, MA, having the least hydrodynamic volume, may be more compact and generate a greater shear force, ultimately leading to a higher Brookfield viscosity.

Furthermore, a gradual decrease in the viscosity with an increase in temperature, 40–100°C (Fig. 2), was observed. In all three polymers, regardless of the composition, intermolecular interactions were reduced with an increase in temperature. P(AN/IA) (14.5 wt %) in DMF at 40°C showed a viscosity of 13,750 cps. However, at 100°C, the viscosity dropped significantly to 1800 cps.

The dope viscosity plays an important role in the spinnability of acrylic fibers. The spinning dope, like other polymer solutions, is viscoelastic, so the fine stream at the exit of the spinneret will be expected to display a die swelling phenomenon. A very low viscosity may lead to dope fracture, whereas a high viscosity may slow down the spinning speed and coagulation rate. Generally, the temperature of the spinning dope is raised to reduce the elastic viscosity, and so there is easy spinning along with reduced die swell.

In this study of spinning, the dope viscosity was kept between 5700 and 6250 cps at 70°C with solid contents of P(AN/MAA) and P(AN/IA) copolymers of 14.5 wt %. As the viscosity of 14.5 wt % P(AN/MA) was very high (7750 cps at 70°C), the dope solids were reduced to 12.6 wt % with a viscosity of 5700 cps at 70°C. The dope temperature of P(AN/IA) was kept at 60°C so that the viscosity was maintained at 6250 cps (Table IV).

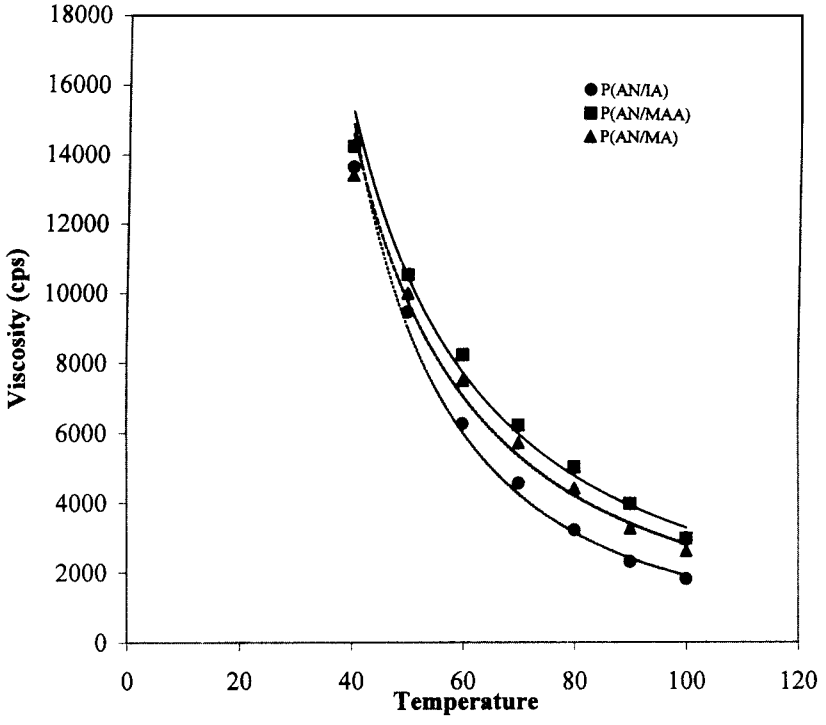

Figure 2 Brookfield viscosity of P(AN/MAA), P(AN/IA), and P(AN/MA) polymers doped at different temperatures.

TABLE V
Mechanical Properties of F(AN/MAA) Fibers at Various Spinning Bath Temperatures and Draw Ratios

Spinning bath temperature (°C)	Draw ratio	Fiber diameter (μm)	Density $(g/cm)^3$	Den/filament	Tenacity (g/den)	Elongation at break (%)	Young modulus (g/den)
	Gel fiber jet stretch = 0.5	45	1.177	17.5	0.43	53	27
	1.1	59	1.194	17.1	0.54	47	24
10	4	36	1.194	2.5	1.69	16	69
	5	23	1.194	2.3	2.09	15	74
	6	16	1.196	2.1	2.23	13	76
	Gel fiber jet stretch = 0.5	50	1.175	17.5	0.34	42	17
	1.1	61		12.9	0.35	39	15
20	4	39		6.8	1.3	12	37
	5	35		6.7	1.74	11	44
	6	34		5.5	2.29	10	85
	Gel fiber jet stretch = 0.5	56	1.171	16.7	0.34	38	19
	1.1	66		12.2	0.35	34	18
30	4	35		5.0	1.38	14	46
	5	30		4.2	1.55	12	52
	6	23		2.8	2.30	12	99
	Gel fiber jet stretch = 0.5	67	1.169	14.3	0.30	32	17
	1.1	87		10.0	0.28	24	13
40	4	41		4.4	0.85	13	30
	5	26		2.7	1.97	13	76
	6	25		2.4	2.30	9.2	92

Effect of the coagulation bath temperature

Diameter and Denier per filament

We measured the fiber diameter to ascertain volumetric changes during spinning. The gel fiber diameter of F(AN/MAA) increased from 45 to 67 μm when the coagulation bath temperature was increased from 10 to 40°C (Table V): at a lower coagulation bath temperature, the outward diffusion of DMF (solvent) predominated, resulting in a reduction in diameter. However, at a higher temperature, the coagulation took place by the counterdiffusion of the solvent and nonsolvent, with an increased influx of water to an outflow of solvent. Interestingly, no die swelling effect was observed in this case, as the process was a dry–jet–wet spinning. Instead, at a 10°C coagulation bath temperature, a decrease in the fiber diameter could be observed. When the spinneret diameter was 50 μm, the gel fiber produced with a 10°C coagulation bath showed a diameter of 45 μm. Moreover, the diameter of the fiber collected from the second bath (10:90 DMF/H_2O, 40°C) was higher than that collected from the first bath (60:40 DMF/H_2O, 10°C). At a 10°C coagulation bath temperature, the gel fiber diameter was 45 μm; when these fibers were taken out from the second bath (10:90 DMF/H_2O, 40°C), the diameter increased to 59 μm. In the second bath, it appears that the higher temperature (40°C) and higher nonsolvent concentration favored the influx of nonsolvent and the bulging of the fiber diameter, which was almost in the coagulated form. Thereafter, the fiber diameter was reduced because of the higher draw ratio. The fiber that was coagulated at 10°C and subsequently drawn to a total draw ratio of 6 had a diameter of 16 μm.

The denier of the fiber decreased with an increase in the coagulation bath temperature and draw ratio. The denier per filament of the gel fiber produced at a 10°C coagulation bath temperature was 17.5, whereas the fiber produced with a 40°C coagulation bath was 14.3. This decrease in the denier with an increase in the coagulation bath temperature might have been due to the porous structure of the gel fiber produced at 40°C.

Cross-sectional shape

The SEM photographs of F(AN/MA), F(AN/MAA), and F(AN/IA) fiber cross sections spun at various temperatures from 10 to 40°C are given in Figures 3–5. The cross-sectional shape of F(AN/MAA) fibers (Fig. 3) changed from a bean shape to an oval and the number of voids increased with the coagulation bath temperature increasing from 10 to 40°C. At 40°C, the fibers were more or less oval and exhibited the maximum number of larger voids. Similar observations have been reported by various researchers.[8,16,24,25]

In the wet spinning of acrylic fibers, there is a transformation of a polymer solution into a solid phase or a porous gel network by the action of the nonsolvent. The polymer/solvent/nonsolvent interactions and the rate at which the changes occur determine the fibrillar network and ultimate fiber properties. A phase separation (coagulation) results in skin formation around the fiber, and this reinforced skin regulates the inter-

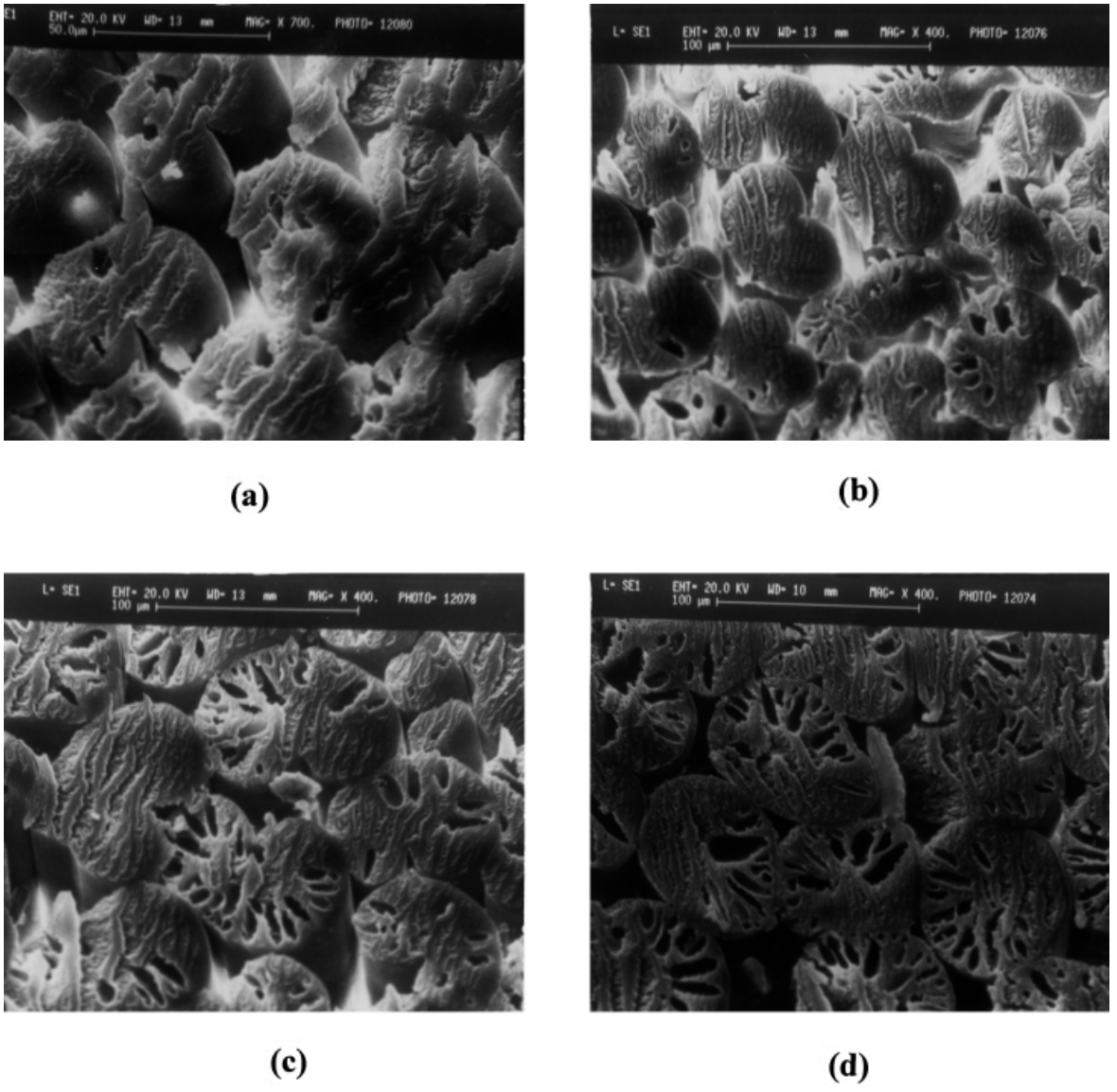

Figure 3 SEM photographs of F(AN/MAA) gel fibers spun at different coagulation bath temperatures: (a) 10, (b) 20, (c) 30, and (d) 40°C.

action between the coagulation bath and the plastic gel within the fiber.

Figure 4 shows the cross-sectional shape of F(AN/MA) gel fibers produced at different coagulation bath temperatures ranging from 10 to 40°C. The gel fiber produced at 10°C was smooth and exhibited very few voids (there was a maximum of two voids per single fiber cross section). MA being a neutral comonomer may hinder inward nonsolvent (H_2O) diffusion and slow coagulation. Because of this, the fibers were kidney-shaped as the outward diffusion of the solvent predominated. Also, the number of voids increased with temperature.

The cross-sectional morphology of the F(AN/IA) fibers at 10–40°C is illustrated in Figure 5. It is entirely different from that of F(AN/MAA) and F(AN/MA) fibers. The cross section changed from a kidney shape to a shoe shape when the coagulation bath temperature was increased from 10°C to 40°C. Instead of voids, there were large fibrillar or lamellar structures horizontal to the cross section. It is evident that the coagulation was a diffusion-controlled, phase-separation process, so the void size and structure were dependent on the rate of coagulation and elongational viscosity of the polymer dope. The dope viscosity of the P(AN/IA) spinning solution was minimal, and the ease of nonsolvent (water) diffusion toward the fiber might have been facilitated to the maximum extent in this case. Also, IA being more hydrophilic might have caused a faster inward diffusion of the nonsolvent, creating a lamellar network structure. For this reason, the F(AN/IA) fibers could be stretched to only a draw ratio of 4, whereas the other two fibers could be stretched to a maximum draw ratio of 6.

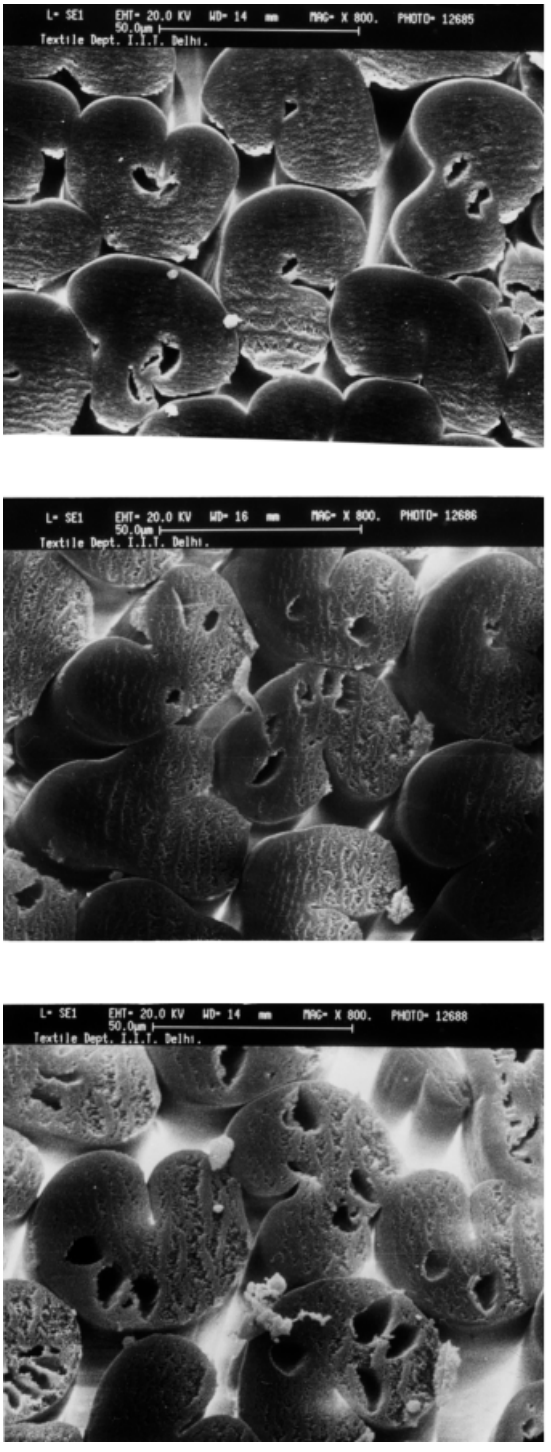

Figure 4 SEM photographs of F(AN/MA) gel fibers spun at different coagulation bath temperatures: (a) 10, (b) 20, and (c) 40°C.

Density

The density of the fibers decreased with an increase in the coagulation bath temperature (Table V) and increased slightly with an increase in the draw ratio. The density of F(AN/MAA) fiber produced at 10°C was 1.177 g cm^{-3}, whereas that produced with a 40°C coagulation bath was 1.169 g cm^{-3} because of the larger voids that formed. It was expected that at a higher coagulation bath temperature, a skin would be formed first and later outward diffusion of the solvent would break open the skin to produce a porous structure. As the fibers were drawn, molecules closely packed and voids collapsed and took a lower volume for the same mass to give an improved density.

Mechanical properties

Gel fibers

The mechanical properties of F(AN/MAA) fibers produced at different coagulation bath temperatures and draw ratios are presented in Table V. The tenacity, modulus, and elongation at break of the gel fibers obtained from first coagulation bath decreased with an increasing coagulation bath temperature. The tenacity of the gel fiber produced at a 10°C coagulation bath temperature was 0.43 g/den, and that at 40°C was 0.30 g/den. Similarly, the modulus dropped from 27 to 17 g/den when the coagulation bath temperature was increased from 10 to 40°C. The percentage elongation at break of the gel fiber also decreased from 53 to 32% with an increase in temperature.

The strength, modulus, and elongation at break of the gel fibers depended largely on the number and size of voids present. It may be recalled that at 40°C, the number and size of the voids of the gel fibers were greater (Fig. 3) than for those obtained at 10°C, so the strength, modulus, and elongation at break of the gel fiber produced at 10°C would be higher than that produced at 40°C, as the voids acted as weak linkages or sites for breakage.

Comparing the mechanical properties of the gel fibers produced from the three different copolymers [P(AN/MAA), P(AN/MA), and P(AN/IA)], we found that the mechanical properties of F(AN/MAA) and F(AN/MA) were similar for a 10°C coagulation bath (Table II). The tenacity of the F(AN/MA) gel fiber at a 10°C coagulation bath temperature was 0.44 g/den. That of F(AN/MAA) under similar conditions was 0.43 g/den, as discussed earlier. Similar behavior was observed for the modulus and elongation at break as well. However, all the properties of the F(AN/IA) gel fibers were inferior, perhaps because of the difference in the phase-separation behavior. The F(AN/IA) gel fiber at a 10°C coagulation bath temperature showed a tenacity of 0.32 g/den, a modulus of 14.3 g/den, and an elongation of 28%. All these values were lower than those of the former two fibers.

At a 40°C coagulation bath temperature, the properties of F(AN/MA) seemed to be better than those of F(AN/MAA) or F(AN/IA). The tenacity, modulus, and elongation at break of F(AN/MA) at 40°C were 0.38 g/den, 17.8 g/den, and 51%, respectively. Under

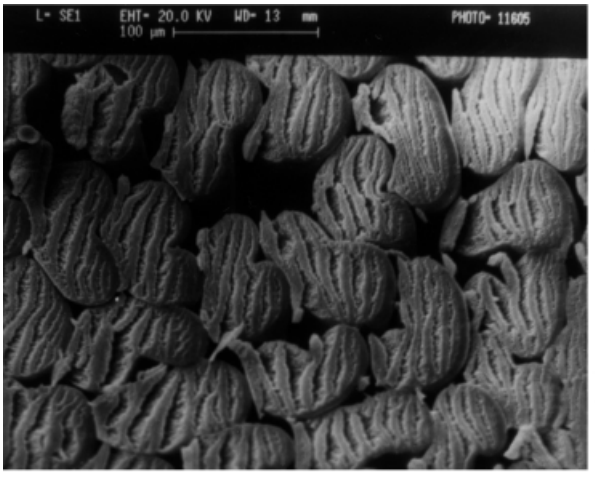

(a)

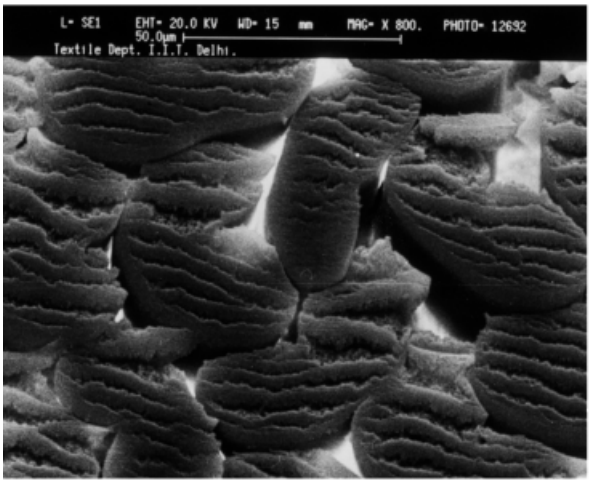

(b)

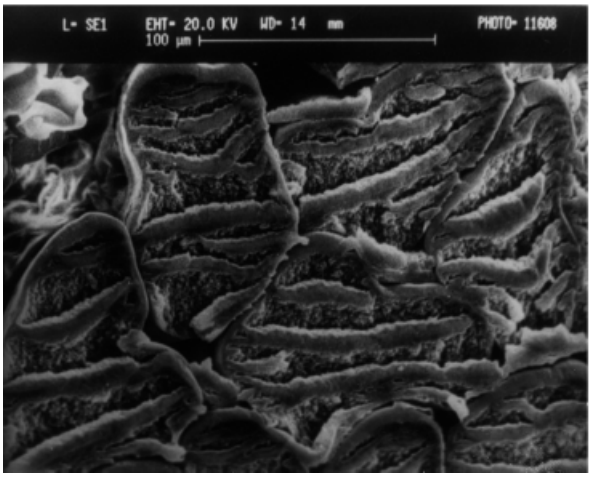

(c)

Figure 5 SEM photographs of F(AN/IA) gel fibers spun at different coagulation bath temperatures: (a) 10, (b) 20, and (c) 40°C.

similar conditions, the tenacity, modulus, and elongation of F(AN/MAA) were 0.30 g/den, 17.0 g/den, and 42%, respectively. The reason may be that MA, being a neutral comonomer, had the least affinity toward water, and the diffusion of water toward the fiber might have been hindered, allowing a slow coagulation. Also, the gel fibers of F(AN/MA) contained fewer voids than F(AN/MAA) (Fig. 4).

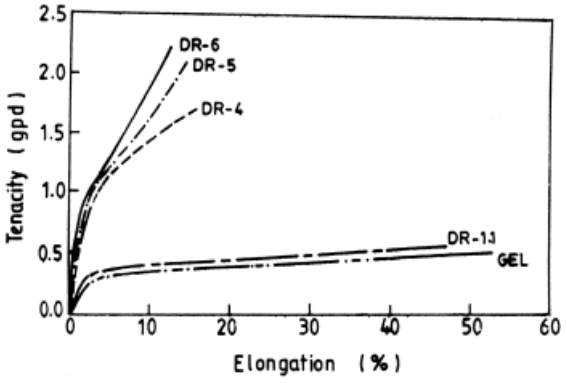

Figure 6 Stress–strain curves of F(AN/MAA) fibers drawn at different temperatures.

Drawn fibers

The strengths of 6× drawn fibers of F(AN/MAA) and F(AN/MA) are nearly the same, between 2.23 and 2.3 g/den, regardless of different coagulation bath temperatures (Table V).

The 6× drawn, collapsed fibers exhibited no voids, and the strength mainly depended on the molecular orientation. When the gel fibers were stretched in boiling water and dried over a heater plate, the fiber diameter was reduced and voids collapsed. However, for the 6× drawn fibers, the modulus showed an increase, and the elongation at break decreased with an increase in the coagulation bath temperature.

The strength and modulus of the fibers increased when the fibers were stretched, regardless of the coagulation bath temperature. At a 10°C coagulation bath temperature, the strength of the F(AN/MAA) gel fiber increased from 0.43 to 2.23 g/den when it was drawn to 6×(Fig. 6). Similarly, the modulus also increased from 27 to 76 g/den. However, the elongation at break decreased from 53 to 13%. When the fibers were stretched, the molecules became oriented toward the fiber axis and contributed toward the total strength.

Table VI shows that the strength and elongation of F(AN/MA) fibers were higher than those of other fibers. The strength and elongation of the 6× drawn F(AN/MA) fiber produced at a 10°C coagulation bath temperature were 2.9 g/den and 14%, respectively, but those of F(AN/MAA) were 2.23 g/den and 13%. However, the modulus was higher for F(AN/MAA) fibers. At a 10°C coagulation bath temperature, the 6× drawn F(AN/MAA) had a modulus of 65 g/den, and that of F(AN/MA) was 55 g/den. Therefore, the incorporation of about 1–2 mol % MA and MAA as comonomers may improve the tenacity, modulus, and elongation at break of the final fibers.

WAXD

One very sharp diffraction at $2\theta = 16.5°$ and a diffuse peak at $2\theta = 28–29°$ were observed in WAXD patterns of drawn and annealed fibers (Fig. 7). For this reason, PAN has been characterized as a single-phase paracrystal with a rodlike structure.[26] The sharpness of both peaks increased with drawing, and $\beta_{1/2}$ decreased. Although for the peak at $2\theta = 16.5°$ the $\beta_{1/2}$ value of the gel fiber was 3°, it was 1.95° for the 6× drawn fiber. The reduction in $\beta_{1/2}$ corresponds to an increase in t_c. t_c increased from 22.9 to 43.4 Å when the gel fiber at 10°C was stretched six times. This indicates that the crystal perfection increased with the draw ratio. Furthermore, the crystal perfection of F(AN/MAA) fibers seemed to be better when the fibers were coagulated at 40°C, as evident from the t_c value of 50.1 Å for the 6× drawn fibers produced at a 40°C coagulation bath temperature (Table VII). However, the χ_c values (61–63%) for a 10°C coagulation bath were not

TABLE VI
Comparison of Mechanical Properties of F(AN/MAA), F(AN/MA), and F(AN/IA) Fibers

	Fiber					
	F(AN/MAA) TDR = 6		F(AN/MA) TDR = 6		F(AN/IA) TDR = 4	
Property	Gel fiber	Final fiber	Gel fiber	Final fiber	Gel fiber	Final fiber
Den/filament						
10°C	17.5	2.1	12.3	2.06	16.3	4.8
40°C	14.3	2.4	11.2	1.87	13.8	4.2
Tenacity (g/den)						
10°C	0.43	2.23	0.44	2.90	0.32	0.83
40°C	0.30	2.30	0.38	3.10	0.24	0.81
Modulus (g/den)						
10°C	27	76	18.2	55.0	14.3	24.8
40°C	17	92	17.8	57.0	14.1	22.0
Elongation (%)						
10°C	53.0	13.0	52.0	14.0	28	8.0
40°C	42.0	9.2	51.0	14.6	26	7.8

TDR = total draw ratio. The molar ratios of the fibers were F(AN/MAA) = 98.7:1.3, F(AN/MA) = 98.7:1.3, and F(AN/IA) = 99.3:0.7.

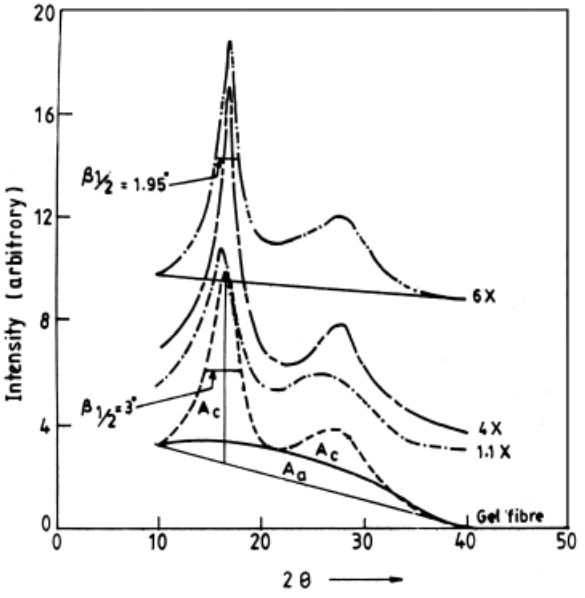

Figure 7 WAXD patterns of drawn F(AN/MAA) fibers of different draw ratios.

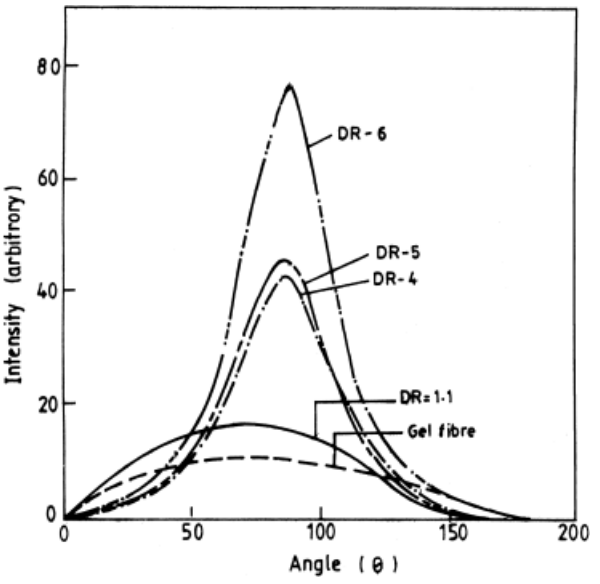

Figure 8 WAXD patterns (azimuthal scan) of drawn F(AN/MAA) fibers.

significantly changed with the draw ratio. χ_c for the acrylic fibers produced at 40°C was less (53–55%) than that for fibers coagulated at 10°C. This might have been because at 10°C the fibers coagulated slowly, and the molecules had more time for a better rearrangement of nitrile dipoles.

The X-ray orientation also increased with an increase in the draw ratio. For fibers produced with a 10°C coagulation bath, the orientation factor increased from 0.41 to 0.78. The X-ray orientation was higher for 40°C coagulated fibers (0.85 for 6× drawn fibers). This shows that the more amorphous nature of the fiber coagulated at 40°C allowed smooth drawing and crystalline orientation.

The azimuthal scans (0–180°) of various drawn and undrawn fibers at $2\theta = 16.5°$ are presented in Figure 8. The intensity of this peak increased with the draw ratio, and $\beta_{1/2}$ decreased.

Sonic modulus

The sonic modulus, an indication of the overall orientation, increased with the draw ratio from 31 to 146 g/den when the gel fibers were stretched to 6× (Table VII). When the gel fibers were drawn to 1.1× in the second bath, there was a slight reduction in the sonic modulus (from 31 to 29 g/den with a 10°C coagulation bath and from 27 to 24 g/den with a 40°C coagulation bath) at 10 and 40°C. As the fiber was taken in the second bath, which was at 40°C with 90% nonsolvent, larger voids were formed, as discussed earlier. The presence of these larger voids obstructed the passage of sound waves, thereby reducing the sonic velocity and sonic modulus. It was more evident from the data that the sonic modulus of the F(AN/MAA) gel fibers that coagulated at a 40°C coagulation bath temperature was lower (27 gpd) than that produced at 10°C because of the greater number of voids.

TABLE VII
WAXD and *E* Data for F(AN/MAA) Fibers at Different Draw Ratios Spun at 10 and 40°C Coagulation Temperatures

Acrylic fiber at different coagulation bath temperatures (°C)	Draw ratio	χ_c (%)	t_c (Å)	X-ray orientation factor	E (g/den)	α
F(AN/MAA) (10°C)	Gel fiber	63	22.9	0.41	31	0
	1.1	62	26.8	0.62	29	—
	4	63	41.1	0.74	58	0.47
	5	63	41.1	0.77	120	0.74
	6	61	43.4	0.78	146	0.79
F(AN/MAA) (40°C)	Gel fiber	53	36.5	0.54	27	0
	1.1	54	35.2	0.42	24	—
	4	54	38.2	0.78	52	0.48
	5	53	50.1	0.83	123	0.78
	6	55	50.1	0.85	134	0.80

The orientation factor calculated from the sonic modulus values also increased with an increase in the draw ratio. The lower value of the sonic modulus orientation factor at a low draw ratio in comparison with the X-ray orientation factor might be due to the crystalline region being more oriented in those samples. However, at a higher draw ratio (6), the X-ray and sonic modulus orientation factors were nearly equal (~0.8). This shows that at a higher draw ratio, both crystalline and amorphous regions contributed equally to the total orientation.

Dichroic ratio

The values of the dichroic ratio of IR absorption bands due to CH, CN, and CO groups in PAN fibers at different draw ratios are given in Table VIII. The dichroic ratio, a measure of molecular orientation, decreased with the draw ratio as expected (Fig. 9). Similar observations were made by Kumar and Stein[22] and Bohn et al.[27] The dichroic ratio of the gel fibers was nearly 1. This shows that the gel fibers were almost unoriented as the absorbances at both parallel and perpendicular directions were equal.

Thermomechanical properties

Figure 10 shows the thermomechanical behavior of 6× drawn F(AN/MAA) and F(AN/MA) fibers and 4× drawn F(AN/IA) fibers. All fibers showed two shrinkage maxima, one between 103 and 134°C and the other around 250°C. These two-step processes may be attributed to physical and chemical shrinkage, respectively. The former occurred because of the relaxation of stresses that built up in the amorphous phase during the fiber spinning and drawing, whereas the second step of thermal shrinkage was due to chemical reactions that led to the cyclization of nitrile groups. Jain et al.[28] explained the physical shrinkage in the coiling of the oriented chains and the shrinkage at the higher temperature side (250°C) on the basis of chemical reactions associated with the nitrile oligomerization leading to ladder polymer formation.

TABLE VIII
Effect of Draw Ratio on the Dichroic Ratio of F(AN/MAA) Acrylic Fibers

Wave number (cm^{-1})	Draw ratio	Dichroic ratio ($A_{\parallel}/A_{\perp}$)
2939 νCH	0	1.03
	1.1	0.98
	4	0.78
	5	0.77
	6	0.75
2240 νC≡N	0	1.01
	1.1	0.96
	4	0.68
	5	0.66
	6	0.64
1732 νC=O	0	0.98
	1.1	1.06
	4	0.90
	5	0.86
	6	0.81

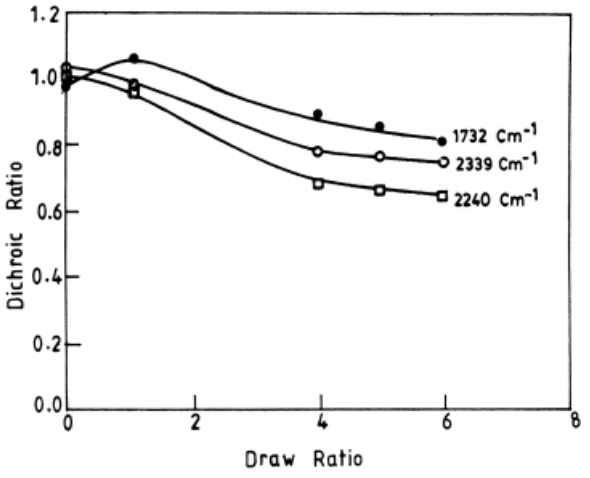

Figure 9 Change in the dichroic ratio of F(AN/MAA) fibers drawn at different steps.

Physical shrinkage

The physical shrinkage of F(AN/IA) with a draw ratio of 4× began at 77.3°C, with a maximum shrinkage at 134°C (Table IX). For F(AN/MAA) fibers, however, the shrinkage began at 58°C. The physical shrinkage may depend on both the stretching during fiber production and the glass-transition temperature. In fact, the onset temperature of physical shrinkage may be considered the glass-transition temperature of these fibers at a 40-mN force. The physical shrinkage maximum (D'_{max}) was between 103 and 134°C (Table IX). The shrinkage in this region was due to the second glass transition associated with the intermolecular interactions of nitrile groups.[29] F(AN/MA) fiber drawn to a 6× draw ratio showed maximum physical shrinkage (51.7%), whereas F(AN/IA) with a 4× draw ratio showed the minimum (30.5%). F(AN/MA) fibers, because of a 6× draw ratio and the presence of MA, might have undergone maximum orientational stretching, and more internal stresses might have built up. Also, F(AN/MA) fibers might have been more amorphous. However, because F(AN/IA) could be drawn only to 4×, it generated less internal stress and showed lower physical shrinkage.

Chemical shrinkage

The chemical shrinkage due to nitrile cyclization took place from 197 to 298°C. The chemical shrinkage max-

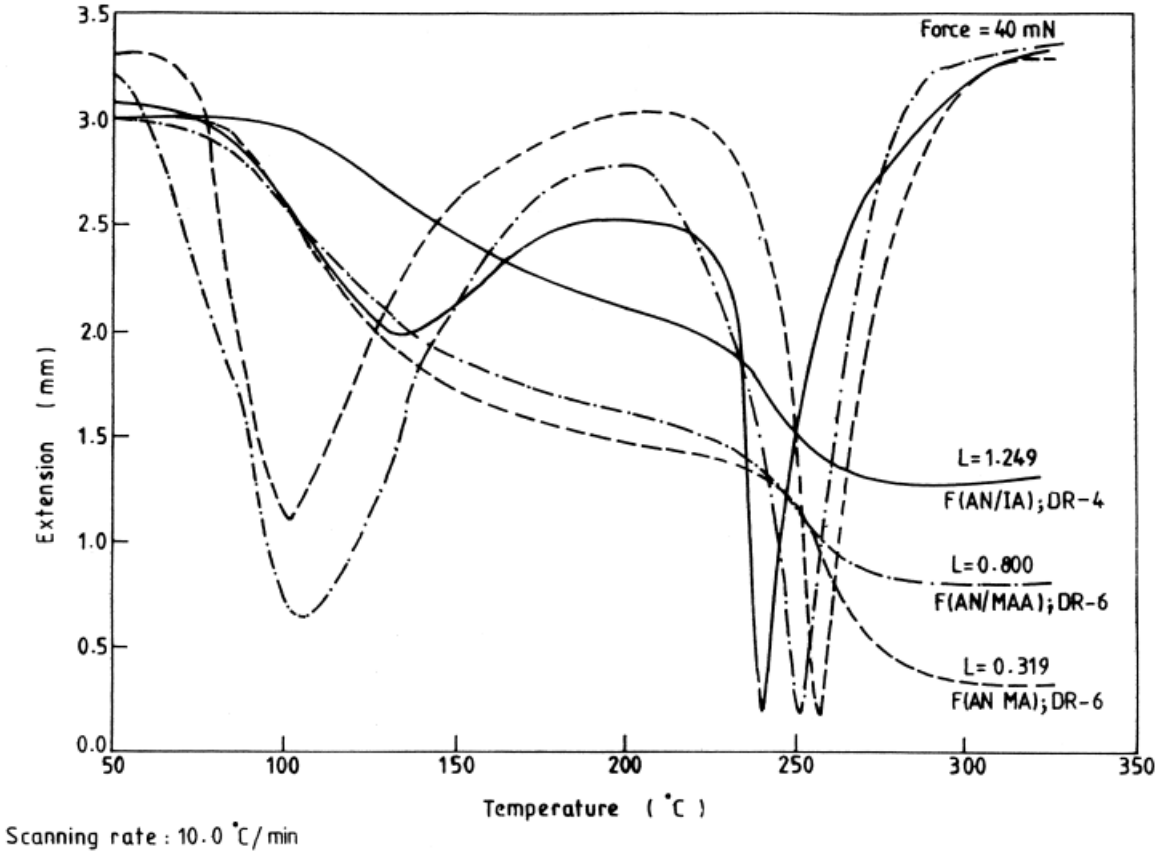

Figure 10 TMA curves of AN copolymer fibers (6× draw ratio).

imum of F(AN/IA) occurred at 239.3°C. For F(AN/MA), this value was 256.7°C, which indicates that the chemical reaction was facilitated in F(AN/IA) copolymers, and the reactions were delayed for F(AN/MA). This was because of the two carboxylic groups of IA, which facilitated the nitrile cyclization better than MAA or MA.

CONCLUSIONS

- The fiber diameter increased and the density decreased with an increase in the coagulation bath temperature.
- At all coagulation bath temperatures (10–40°C), F(AN/MAA) and F(AN/MA) showed mainly circular voids. However, F(AN/IA) showed large lamellar network structures horizontal to the fiber cross section; because of this morphology, these fibers could be drawn only to a 4× draw ratio.
- The 6× drawn final fibers showed similar tenacity, regardless of the coagulation bath temperature.
- The tenacity and elongation of drawn and annealed F(AN/MA) fibers were better than those of F(AN/MAA) and F(AN/IA) fibers. However, the initial modulus was better for F(AN/MAA) fibers.
- The crystal size and orientation increased with an increase in the draw ratio. However, the crystallinity was not affected with stretching.
- The sonic modulus increased with an increase in the draw ratio and decreased with an increase in voids.
- The dichroic ratio decreased with an increase in the draw ratio.

TABLE IX
Thermomechanical Data of AN Copolymer

Fiber	Draw ratio	Physical shrinkage		D'_{max} (physical; °C)	Chemical shrinkage		D'_{max} (chemical; °C)	Total shrinkage (%)
		Temperature range (°C)	Shrinkage (%)		Temperature range (°C)	Shrinkage (%)		
F(AN/IA)	4	77.3–202.0	30.5	134	202–290	27.8	239.3	58.3
F(AN/MAA)	6	58–196.7	47.1	103	196.7–298	26.2	250.7	73.3
F(AN/MA)	6	70–203.3	51.7	125.3	203.3–286	37.6	256.7	89.3

REFERENCES

1. Bajaj, P. In Progress in Textile Science; Kothari, V. K., Ed.; IAFL: 2000; Vol. 2, Chapter 10, pp 539–601.
2. Gupta, A. K.; Paliwal, D. K.; Bajaj, P. J Macromol Sci Rev Macromol Chem Phys 1991, 31, 1.
3. Sen, K.; Baharami, S. H.; Bajaj, P. J Macromol Sci Rev Macromol Chem Phys 1996, 36, 1.
4. Bajaj, P.; Roopanwal, A. K. J Macromol Sci Rev Macromol Chem Phys 1997, 37, 97.
5. Mitsubishi Rayon Co., Ltd. Chem Abstr 1988, 109, 7918h.
6. Toray Industries, Inc. Chem Abstr 2000, 132, 51087k.
7. Bajaj, P. In Manufactured Fibre Technology; Gupta, V. B.; Kothari, V. K., Eds.; Chapman & Hall: London, 1997; Vol. 1, Chapter 15, pp 406–504.
8. Knudsen, J. P. Textile Res J 1963, 33, 13.
9. Prasad, G. Man-Made Textiles India 1985, 28, 57.
10. Mamazhanov, A. A.; Timoshina, L. V.; Zakirov, I. Z.; Ergashev, K. E.; Askarov, M. A. Khim Volokna 1990, 4, 22.
11. Bajaj, P.; Sreekumar, T. V.; Sen, K. J Appl Polym Sci 2001, 79, 1642.
12. Qingly, J.; Wangxi, Z.; Jianjan, L.; Huasn, C. Gaofenzi Xueabao 1999, 5, 640; Chem Abstr 2000, 132, 36890y.
13. Mitsubishi Rayon Co., Ltd. Chem Abstr 1988, 109, 7938q.
14. Wilkinson, K. Chem Abstr 1997, 126, 105398j.
15. Takahashi, M.; Nukushina, Y.; Kosugi, S. Text Res J 1964, 34, 87.
16. Bell, J. P.; Dumbleton, J. H. Textile Res J 1971, 41, 196.
17. Bajaj, P.; Munukutla, S. K.; Vaidya, A. A.; Gupta, D. C. Textile Research Journal, Oct 1989, p 601.
18. Bajaj, P.; Kumari, S. K. Textile Res J 1989, 59, 191.
19. Capone, G. J. In Acrylic Fibre Technology and Applications; Masson, J. L., Ed.; Marcel Dekker: New York, 1995; Chapter 4, pp 69–103.
20. Baojan, Q.; Jian, Q.; Zhenlong, Z. Textile Asia 1989, 20, 48.
21. Nikkiso Co., Ltd. Chem Abstr 1989, 111, 116748b.
22. Kumar, S.; Stein, R. S. J Appl Polym Sci 1982, 27, 3407.
23. Paul, D. R. J Appl Polym Sci 1969, 13, 817.
24. Bajaj, P.; Sreekumar, T. V.; Sen, K. Chem Fibre Int 1998, 48, 308.
25. Caig, J. P.; Kundsen, J. P.; Holland, V. F. Text Res J 1962, 32, 435.
26. Hinrichsen, G. J Appl Polym Sci 1973, 17, 3305.
27. Bohn, C. R.; Schaefgen, J. R.; Statton, W. O. J Polym Sci 1961, 55, 531.
28. Jain, M. K.; Balasubramanian, M.; Desai, P.; Abhiraman, A. S. J Mater Sci 1987, 22, 301.
29. Bajaj, P.; Sreekumar, T. V.; Sen, K. Polymer 2001, 42, 1707.